



Cu(II), Co(II) and Ni(II) complexes of new Schiff base ligand: Synthesis, thermal and spectroscopic characterizations

Moamen S. Refat^{a,b,*}, Mohamed Y. El-Sayed^c, Abdel Majid A. Adam^b

^a Department of Chemistry, Faculty of Science, Port Said University, Port Said, Egypt

^b Department of Chemistry, Faculty of Science, Taif University, 888 Taif, Saudi Arabia

^c Department of Chemistry, Faculty of Science, Zagazig University, Egypt

HIGHLIGHTS

- ▶ Three novel bi- or tridentate Schiff base complexes of Cu(II), Co(II) and Ni(II) have synthesized.
- ▶ The calcinations of the Cu(II), Co(II) and Ni(II)–H₂L at 600 °C have succeeded in synthesized nano-structured oxides.
- ▶ The particles deposited at calcinations temperature is in the region of 250–480 nm.

ARTICLE INFO

Article history:

Received 9 November 2012

Received in revised form 22 January 2013

Accepted 24 January 2013

Available online 31 January 2013

Keywords:

Schiff base

Nano-particles

Transition metals

Thermal analysis

ABSTRACT

Cu(II), Co(II), and Ni(II) complexes were synthesized from 2-[(5-*o*-chlorophenylazo-2-hydroxybenzylidene)amino]-phenol Schiff base (H₂L). Metal ions coordinate in a tetradentate or hexadentate features with these O₂N donor ligand, which are characterized by elemental analyses, magnetic moments, infrared, Raman laser, electronic, and ¹H NMR spectral studies. The elemental analysis suggests the stoichiometry to be 1:1 (metal:ligand). Reactions with Cu(II), Co(II) and Ni(II), resulted [Cu(H₂L)(H₂O)₂(Cl)]Cl, [Co(H₂L)(H₂O)₃]Cl₂·3H₂O and [Ni(H₂L)(H₂O)₂]Cl₂·6H₂O. The thermal decomposition behavior of H₂L complexes has been investigated by thermogravimetric analysis (TG/DTG) at a heating rate of 10 °C min⁻¹ under nitrogen atmosphere. The brightness side in this study is to take advantage for the preparation and characterizations of single phases of CuO, CoO and NiO nanoparticles using H₂L complexes as precursors via a solid-state decomposition procedure. The crystalline structures of products using X-ray diffractometer (XRD), morphology of particles by scanning electron microscopy (SEM), energy-dispersive X-ray spectroscopy (EDX) were investigated.

© 2013 Elsevier B.V. All rights reserved.

1. Introduction

Schiff base compounds with the azomethine group (–RC=N–) are usually formed by the condensation of amine –NH₂ group with active –C=O carbonyl group [1]. The field of Schiff bases is fast developing because of the wide variety and potential applications of their industrial, biological, analytical, medicinal, pharmaceutical and catalytical applications [2–7]. Complexes of Schiff bases with some transition metals show significant biological notification including antimicrobial, antibacterial, antifungal and anticancer activities [7–10]. In recent years [11–15] a number of research articles have been published on transition metal complexes of Cu(II), Co(II), Ni(II), Fe(III), Zn(II) with Schiff bases derived from the condensation of salicylaldehyde and *o*-amino phenol or 2-ami-

no benzoic acid. Azo compounds have been studied widely because of their excellent thermal, antibacterial activity and optical properties in applications such as optical recording medium, toner, ink-jet printing and oil-soluble lightfast dyes [16–19].

Based on the previous considerations, we are initiating a line of investigation on the coordination chemistry of Schiff base compounds containing azo group attached with organic moieties. In this paper, we report the characterization by elemental analysis, magnetic properties, infrared spectra (IR), Raman laser, ultraviolet and visible spectra (UV–Vis), X-ray diffraction, scanning electron microscopy, proton nuclear magnetic resonance (¹H NMR), and mass spectra of 2-[(5-*o*-chlorophenylazo-2-hydroxybenzylidene)amino]-phenol Schiff base (H₂L) and its Cu(II), Co(II) and Ni(II) complexes. Thus, the complexes have been isolated and there are well characterized. The ligand H₂L acts as tridentate through two oxygen atoms and nitrogen atom of *o*-aminophenol and salicylaldehyde rings, respectively, for Cu(II) and Co(II) complexes. On the other hand, H₂L acts as bidentate through two oxygen atoms for

* Corresponding author at: Department of Chemistry, Faculty of Science, Port Said University, Port Said, Egypt. Tel.: +966 561926288.

E-mail address: msrefat@yahoo.com (M.S. Refat).

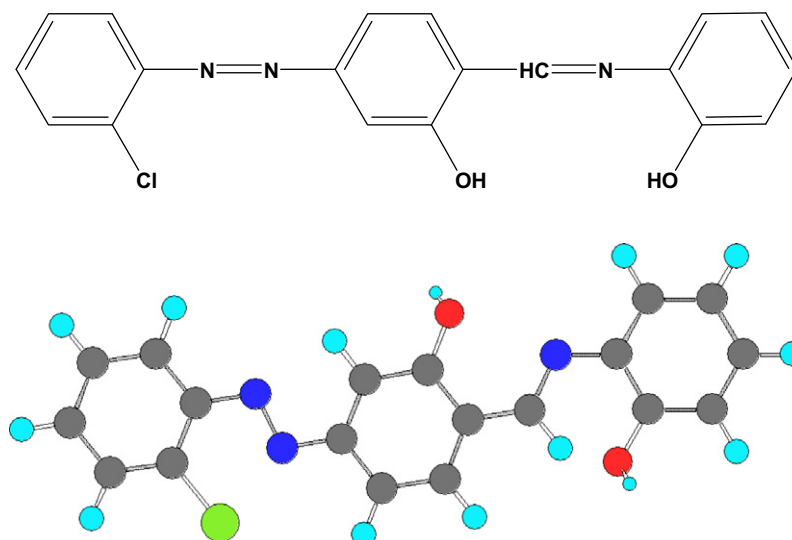


Fig. 1. The structural formula of H₂L Schiff base ligand.

Table 1

Analytical and physical data for H₂L Schiff base and their metal complexes.

Compound Empirical formula (M. Wt.)	Color	λ_m ($\Omega^{-1} \text{ cm}^2 \text{ mol}^{-1}$)	Elemental analysis (%) found (Calcd.)				
			C	H	N	Cl	M
H ₂ L[C ₁₉ H ₁₄ N ₃ O ₂ Cl] (351.5)	Dark red	30	64.80(64.86)	3.95(3.98)	11.92(11.95)	10.08(10.10)	–
[Cu(H ₂ L)(H ₂ O) ₂ (Cl)]Cl (522.05)	Dark green	75	43.14(43.67)	3.38(3.45)	8.00(8.04)	20.09(20.11)	12.13(12.17)
[Co(H ₂ L)(H ₂ O) ₃]Cl ₂ ·3H ₂ O (589.43)	Dark brown	146	38.54(38.68)	4.36(4.41)	7.09(7.13)	17.87(18.07)	9.80(10.00)
[Ni(H ₂ L)(H ₂ O) ₂]Cl ₂ ·6H ₂ O (625.2)	Orange yellow	163	36.45(36.47)	4.78(4.80)	6.65(6.72)	16.97(17.03)	9.28(9.39)

Ni(II) complex. The Cu(II), Co(II) and Ni(II) oxides nanostructures are collected through thermal decomposition process of H₂L complexes which has many advantages like controlling on the process conditions, particle size, particle crystal structure, decreasing the calcinations temperature, and purity.

2. Experimental

2.1. Reagents

o-Chloroaniline, *o*-aminophenol, and salicylaldehyde were obtained from Porlabo. All chemicals used for the study were of analytically reagent grade and used without previous purification as transition metal salts NiCl₂·6H₂O, CoCl₂·6H₂O, CuCl₂·2H₂O and other chemicals. Double distilled water, methanol and diethyl ether solvents were used.

2.2. Synthesis of Schiff base ligands

The ligand, 2-[(5-*o*-chlorophenylazo-2-hydroxybenzylidene)amino]-phenol Schiff base (H₂L) (Fig. 1) was obtained by a procedure in two steps as follows.

2.2.1. Synthesis of 5-arylo-2-hydroxybenzylidene compound (diazotization and coupling processes)

5-Arylo-2-hydroxybenzylidene compound was prepared by dissolving *o*-chloroaniline (50 mmol) in 6.0 mL of hydrochloric acid with concentration 37% and distilled water (30 mL). The solution was then cooled to 0–5 °C in ice-bath and maintained at this temperature. Sodium nitrite (40 mmol, 2.8 g) solution in distilled water (30 mL) was then added dropwise. Stirring was continued for 30 min to produce diazonium salt at the same temperature. The

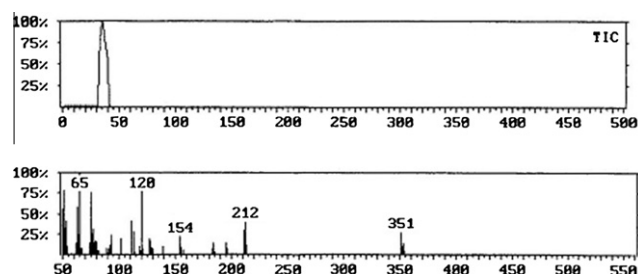
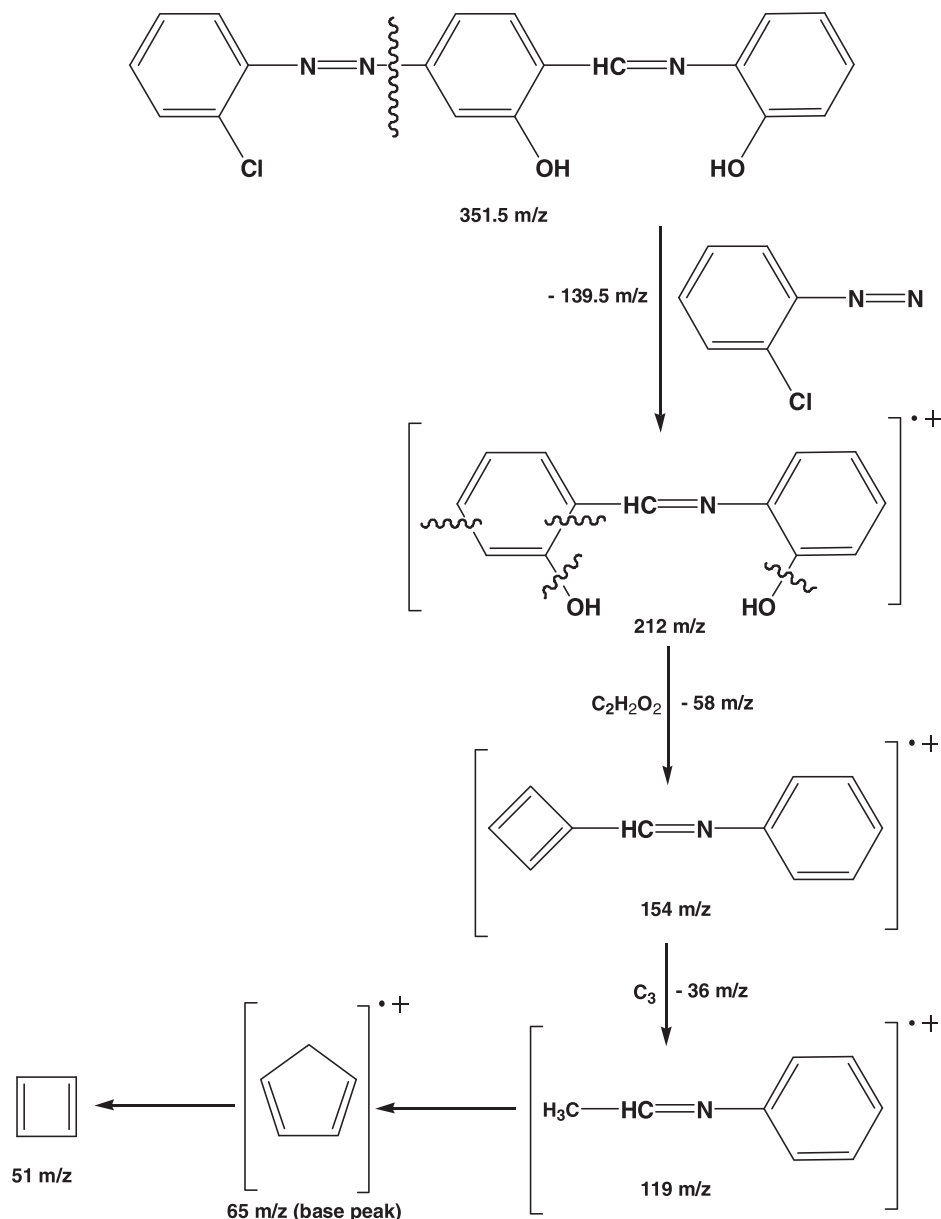


Fig. 2. Mass spectrum of H₂L Schiff base ligand.

diazonium solution was coupled with salicylaldehyde in alkaline media at the *para* position to the hydroxyl group. During the procedure the pH value was maintained within 7–9, and the temperature at 0–5 °C [20]. The mixture was recrystallized several times; the pH value was decreased to ~3, and then left overnight. The precipitate was collected by filtration, washed with small portion of diethyl ether to extract all organic impurities, and then dried under vacuum at 70 °C. The purity of the diazo compound was evaluated by thin layer chromatography.

2.2.2. Synthesis of the H₂L Schiff base ligand

The Schiff base (H₂L) was prepared by mixing 50 mL methanol solution of *o*-aminophenol (50 mmol) with a solution of 5-arylo-2-hydroxybenzylidene (50 mmol) in water (100 mL) under reflux for 2 h. at 70 °C on a hot plate [21]. After cooling, the precipitate was filtered, washed several times with methanol and diethyl ether to remove all organic impurities, dried *in vacuo* over calcium chloride. The purity of the ligand was evaluated by thin layer chromatography and the composition was confirmed by elemental analysis CHN, and (IR, mass, and ¹H NMR) spectra.



Scheme 1. The fragmentation pattern proposed for 2-[(5-*o*-chlorophenylazo-2-hydroxy benzylidene)amino]-phenol Schiff base (H₂L).

Table 2

Assignments of the IR and Raman Spectral bands (cm⁻¹) for H₂L Schiff base and their metal complexes.

Compound	V _(OH)		V _{C=N}		V _{N=N}		V _{C=O}		V _{M-N}		V _{M-O}	
	IR	Raman	IR	Raman	IR	Raman	IR	Raman	IR	Raman	IR	Raman
H ₂ L	3420	-	1620	1591	1464	1415	1205	1256	-	-	-	-
[Cu(H ₂ L)(H ₂ O) ₂ (Cl)]Cl	3162	3249	1603	-	1468	1424	1179	1161	678	573	506	458
[Co(H ₂ L)(H ₂ O) ₃]Cl ₂ ·3H ₂ O	3180	3319	1601	-	1466	1407	1151	1205	666	581	586	511
[Ni(H ₂ L)(H ₂ O) ₂]Cl ₂ ·6H ₂ O	3065	3073	1618	1591	1465	1424	1152	1186	672	573	517	511
									552		480	

2.3. Synthesis of complexes

To a hot solution (1 mmol) of H₂L Schiff base ligand in (30 mL) methanol, a hot solution of corresponding metal(II) salts (Ni²⁺, Co²⁺, Cu²⁺) (1 mmol, in 30 mL methanol) were added slowly. The resulting mixtures were stirred and refluxed on a hot plate at

70 °C for 2 h, and then concentrated to half its initial volume. After cooling for the mixtures overnight, the solid complexes are precipitated and separated, washed with methanol and diethyl ether. The synthesized complexes were recrystallized from methanol and dried under vacuum over anhydrous CaCl₂. The purity was checked by thin layer chromatography.

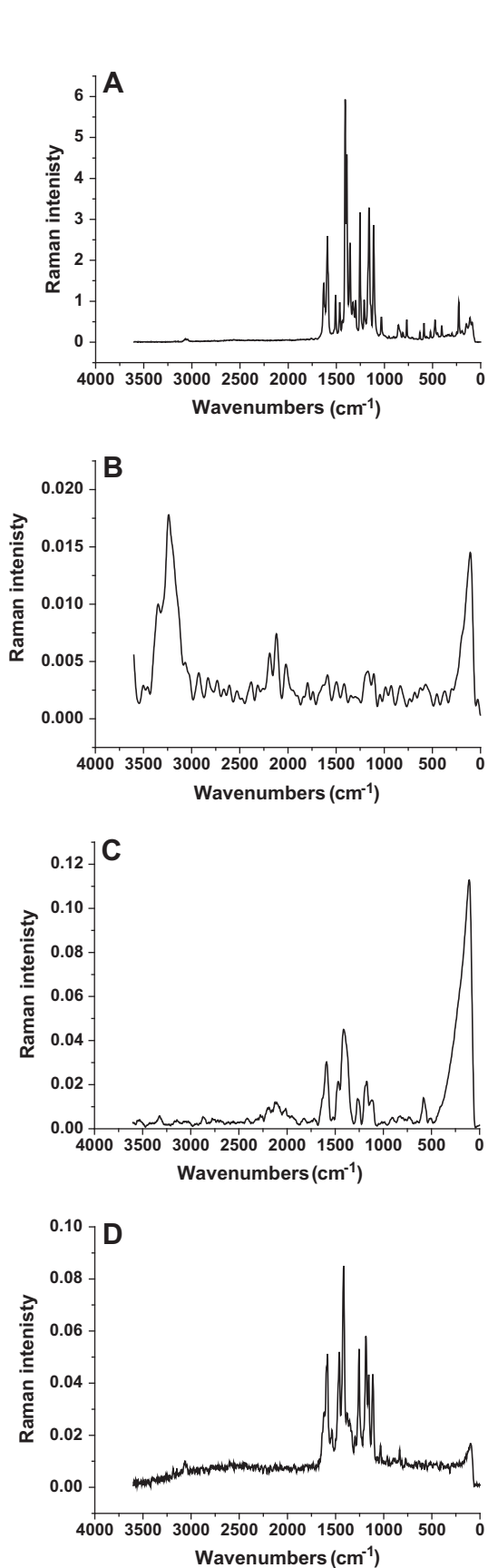


Fig. 3. Raman spectra of H₂L, Cu(II), Co(II) and Ni(III) H₂L complexes (A, B, C and D, respectively).

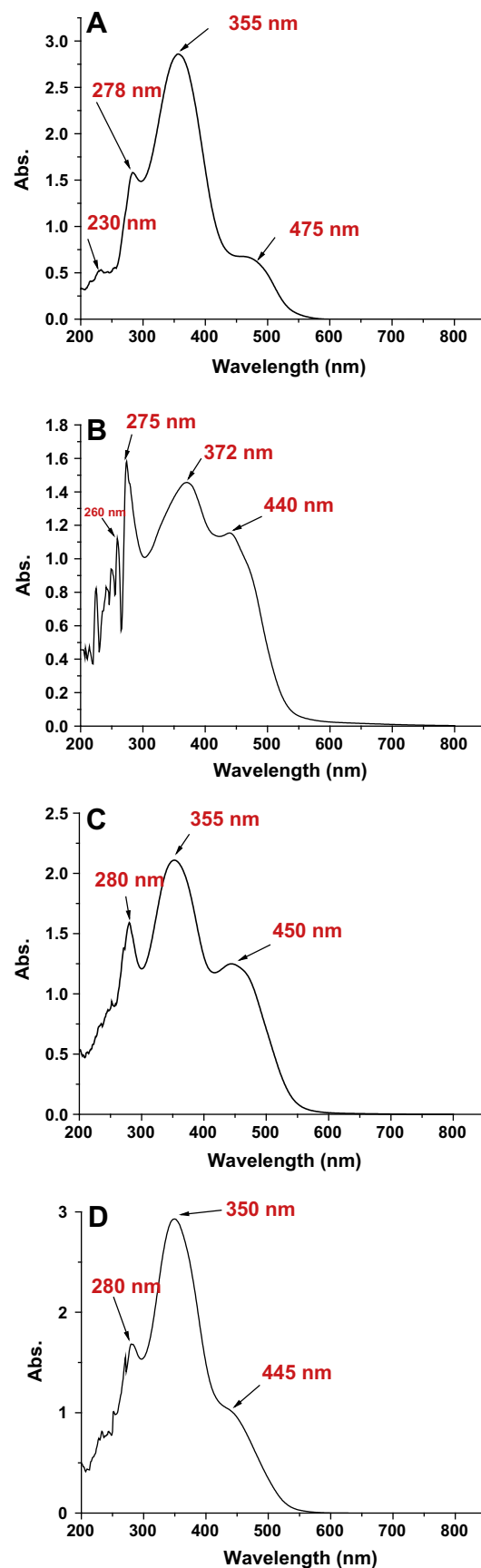


Fig. 4. Electronic spectra of H₂L, Cu(II), Co(II) and Ni(III) H₂L complexes (A, B, C and D, respectively).

Table 3
Electronic spectral bands (cm^{-1}) and magnetic moments of the H_2L ligand and their complexes.

Compound	Magnetic moments μ_{eff}	Electronic spectral values (cm^{-1})	Proposed geometry
H_2L	–	21,052, 28,169, 35,971, 43,478	–
$[\text{Cu}(\text{H}_2\text{L})(\text{H}_2\text{O})_2(\text{Cl})]\text{Cl}$	1.76	22,727, 26,881, 36,363, 38,461, 44,444	Octahedral
$[\text{Co}(\text{H}_2\text{L})(\text{H}_2\text{O})_3]\text{Cl}_2 \cdot 3\text{H}_2\text{O}$	3.89	22,222, 28,169, 35,714	Octahedral
$[\text{Ni}(\text{H}_2\text{L})(\text{H}_2\text{O})_2]\text{Cl}_2 \cdot 6\text{H}_2\text{O}$	–	22,472, 28,571, 35,714	Square planar

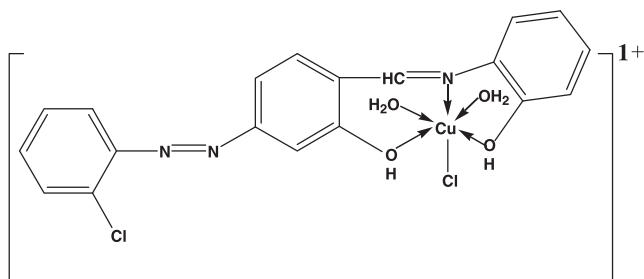


Fig. 5. Suggestion structure of $[\text{Cu}(\text{H}_2\text{L})(\text{H}_2\text{O})_2(\text{Cl})]\text{Cl}$ complex.

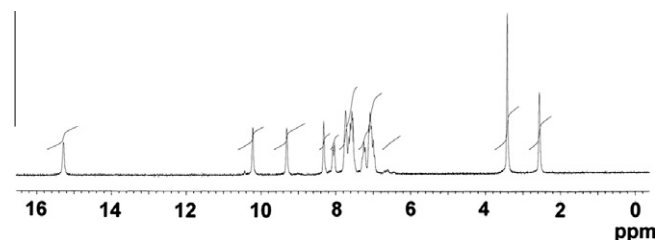


Fig. 8. ^1H NMR spectrum of H_2L Schiff base ligand.

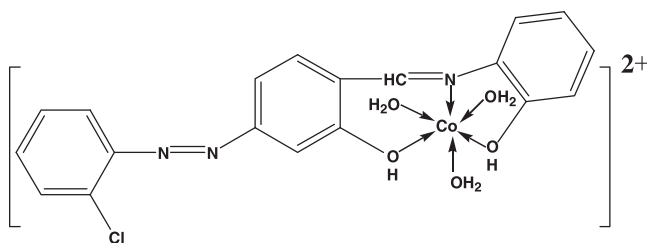


Fig. 6. Suggestion structure of $[\text{Co}(\text{H}_2\text{L})(\text{H}_2\text{O})_3]\text{Cl}_2 \cdot 3\text{H}_2\text{O}$ complex.

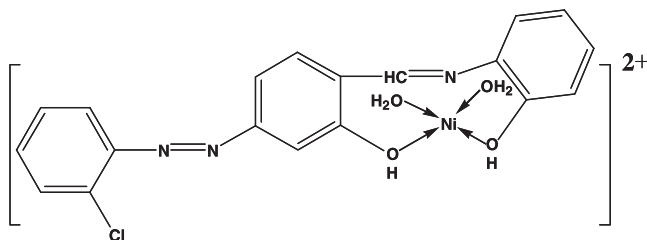


Fig. 7. Suggestion structure of $[\text{Ni}(\text{H}_2\text{L})(\text{H}_2\text{O})_2]\text{Cl}_2 \cdot 6\text{H}_2\text{O}$ complex.

2.4. Equipments

Carbon, hydrogen and nitrogen were analyzed at the Microanalytical unit of Cairo University by a Perkin–Elmer CHN 2400 elemental analyzer. The metal contents were determined gravimetrically by converting the compounds to its corresponding oxides. The chloride ions were gravimetrically determined using a standard method [22] and the data reflect the high conformity with that theoretically proposed. The molar conductivities of freshly prepared 1.0×10^{-3} mol/cm³ dimethylsulfoxide solutions were measured for the soluble complexes using Jenway 4010 conductivity meter. The magnetic measurements were performed using magnetic susceptibility balance Sherwood Scientific Cambridge, England. The infrared spectra, as KBr discs, were recorded on a Bruker FT-IR Spectrophotometer ($4000\text{--}400\text{ cm}^{-1}$) at Cairo University, while Raman laser spectra of samples were measured on the Bruker FT-Raman with laser 50 mW. The electronic and ^1H NMR (200 MHz) spectra were recorded on Perkin–Elmer Pre-

cisely Lambda 25 UV/Vis double beam Spectrometer fitted with a quartz cell of 1.0 cm path length, and a Varian Gemini Spectrophotometers, respectively at Taif (Saudi Arabia) and Cairo universities. The thermal studies were carried out on a Shimadzu thermogravimetric analyzer at a heating rate of $10\text{ }^\circ\text{C min}^{-1}$ under nitrogen till $600\text{ }^\circ\text{C}$ in Cairo University. The purity of H_2L Schiff base ligand was checked via mass spectra at 70 eV by using AEI MS 30 mass spectrometer at room temperature. The X-ray diffraction patterns for the three final decomposition products were recorded on Bruker AXS configuration X-ray powder diffraction. Scanning electron microscopy (SEM) images and Energy Dispersive X-ray Detection (EDX) were taken in Joel JSM-6390LA equipment, with an accelerating voltage of 20 kV.

3. Results and discussion

The percentage (%) of carbon, hydrogen, nitrogen and chloride contents as well as some physical values is tabulated in Table 1. All the isolated of H_2L complexes are stable in air, having high melting points ($>300\text{ }^\circ\text{C}$), insoluble in H_2O and most organic solvents except DMSO and DMF soluble with gently heating. The molar conductivity measurements for (1.0×10^{-3} mol) in DMSO solvent are found within the highly conducting feature for cobalt(II) and nickel(II) H_2L complexes but the copper(II) complex is slightly conducting [23]. The conductivity feature of $\text{M}\text{--}\text{H}_2\text{L}$ complexes belongs to positively charged coordination sphere ionically attached with two (for Co(II) and Ni(II)) or one (for Cu(II)) conjugated chloride anion in the investigated complexes. This phenomenon in agreement with the analytical data which suggest the presence of chloride anion covalently or ionically attached with the central metal ions in $\text{M}\text{--}\text{H}_2\text{L}$ complexes.

3.1. Mass spectral analysis

Mass spectrometry has been successfully used to confirm the molecular ion peaks of H_2L Schiff base and investigate the fragment species. The fragment pattern of mass spectrum gives an impression for the successive degradation of the target compound with the series of peaks corresponding to various fragments. Also, the peaks intensity gives an idea about the stability of fragments especially with the base peak. The recorded mass spectrum of H_2L ligand (Fig. 2) reveals molecular ion peak confirms strongly the proposed formula. The spectrum of the ligand having peak at

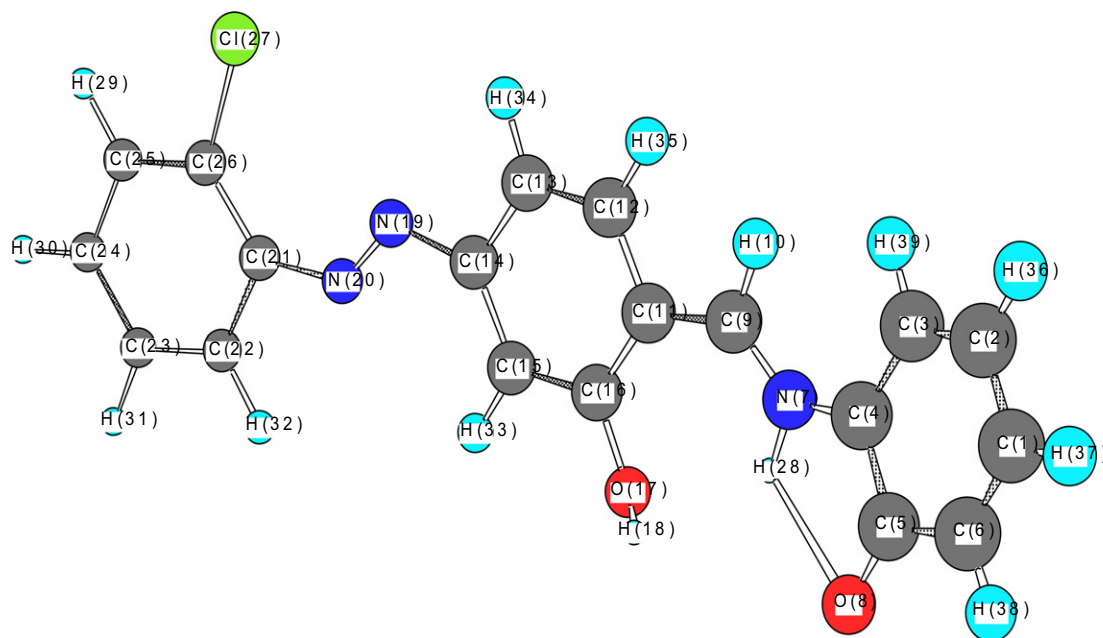


Fig. 9. Hydrogen bonding between OH and nitrogen of azomethine group.

$m/z = 351$ (27%) which is referring to the molecular ion peak (M^+) and confirming the purity of the ligand prepared. The degradation pattern have prominent peaks at $m/z = 212$ (39%), 154 (22%), 120 (80%) and 65 (100%) as displayed in degradation Scheme 1.

3.2. IR and Raman spectral analyses

The distinguish IR spectra (Table 2) provide valuable information regarding the nature of the functional group attached to the metal atom [14,15]. The IR spectra of ligand and its complexes are found to be quite complex as they in general exhibit large number of bands of varying intensities. The spectrum of the free Schiff base ligand shows the peak of azomethine group $-\text{CH}=\text{N}$ at 1620 cm^{-1} , which is shifted to lower frequencies in the spectra of both copper(II) and cobalt(II) complexes at 1603 and 1601 cm^{-1} , respectively, indication the involvement of the $-\text{CH}=\text{N}$ nitrogen in the coordination to metal ion [14]. Concerning nickel(II) complex, the azomethine group located at the same place of H_2L Schiff base ligand (1618 cm^{-1}), this ascribe to the non-participation of azomethine group in the chelation process. Coordination of the Schiff base to the metal ions through the nitrogen atom is expected to reduce the electron density in the azomethine link and lowers the stretching vibrational motion of $\nu(\text{C}=\text{N})$. In the IR spectrum of ligand (H_2L), $\nu(\text{OH})$ band appeared at 3420 cm^{-1} . This band is shifted to lower frequency at 3162 , 3180 , and 3065 cm^{-1} , respectively, in the Cu(II), Co(II) and Ni(II) complexes. The band appearing at the frequency of 1464 cm^{-1} in the spectrum of ligand assigned to $-\text{N}=\text{N}-$ group not affected in the complexes indicates non-participation of azo nitrogen in coordination with metal ions. The phenolic $\text{C}-\text{O}$ stretching vibrations appeared at $\sim 1204\text{ cm}^{-1}$ in the Schiff base under a shift towards lower frequencies ($25\text{--}53\text{ cm}^{-1}$) in the complexes (Table 2). This shift confirms the participation of oxygen in the $\text{C}-\text{O}-\text{M}$ bond [24,25]. The weak-to-very weak bands in the two ranges ($678\text{--}536\text{ cm}^{-1}$) and ($586\text{--}455\text{ cm}^{-1}$), respectively, are assigned to the stretching frequencies of the $\nu(\text{M}-\text{O})$ [26] and $\nu(\text{M}-\text{N})$ [26] bands, which confirmed the attached of H_2L ligand to the center metal ions through the phenolic oxygen atoms and the azomethine nitrogen. The spectra of H_2L

complexes exhibited a broad band around $3414\text{--}3365\text{ cm}^{-1}$, which is assigned to water molecules, $\nu(\text{OH})$, associated with the complexes. In addition to these modes, coordinated water exhibited $\delta_r(\text{H}_2\text{O})$ rocking near $831\text{--}893\text{ cm}^{-1}$ and $\delta_w(\text{H}_2\text{O})$ wagging near $550\text{--}530\text{ cm}^{-1}$ [26]. In the copper(II) complex, the $\nu(\text{Cu}-\text{Cl})$ band cannot easily detected due to the wavenumber scanning range ended at $\sim 400\text{ cm}^{-1}$ which do not includes the value of terminal $\text{Cu}-\text{Cl}$ band rather than bridging chlorine [26].

Fig. 3 shows that the most intense Raman lines in the spectra of H_2L and its Cu(II), Co(II) and Ni(II) complexes were observed at region $3070\text{--}3320\text{ cm}^{-1}$, these lines were assigned to vibrational modes of $\nu(\text{OH})$ Table 2. Furthermore, the other very-medium intense Raman lines observed at (1161 , 1205 , 1186 cm^{-1}), (573 , 581 , 573 cm^{-1}), (458 , 511 , 511 cm^{-1}) in the spectra of Cu(II), Co(II) and Ni(II) complexes, respectively, were assigned to that $\nu(\text{C}-\text{O})$, $\nu(\text{M}-\text{N})$ and $\nu(\text{M}-\text{O})$. These show the effect of complexation via phenolic oxygen and azomethine nitrogen in shifting a number of stretching modes to lower frequencies comparable to free ligand. The Raman line observed at 371 cm^{-1} in case of copper(II) complex was assigned to the stretching vibration of $\nu(\text{Cu}-\text{Cl})$.

3.3. Electronic spectral analysis and magnetic measurements

The data of electronic spectrum of free H_2L Schiff base ligand (Fig. 4, Table 3) was collected in DMSO solvent with four absorption bands at 475 , 355 , 278 and 230 nm . The spectral bands at 230 and 278 nm were assigned to transition motions of phenyl rings [27,28]. The transition band at 355 nm corresponded to $n \rightarrow \pi^*$ transition of azomethine group $-\text{CH}=\text{N}$, while, the band at 475 nm assigned to $n \rightarrow \pi^*$ transitions of donating atoms like oxygen and nitrogen which are overlapped with the intermolecular L_{CT} from aromatic rings. The peaks within the transition motions of phenyl rings have been relatively unaffected in the spectra of the complexes; this is expected for the relatively unshared of aromatic ring in chelation. The transition bands up to 350 nm which assigned to $n \rightarrow \pi^*$ transition due to involving molecular orbitals of the $-\text{CH}=\text{N}$ chromophore. The bands of $n \rightarrow \pi^*$ transition have been shifted upon complexation of H_2L ligand towards all metal

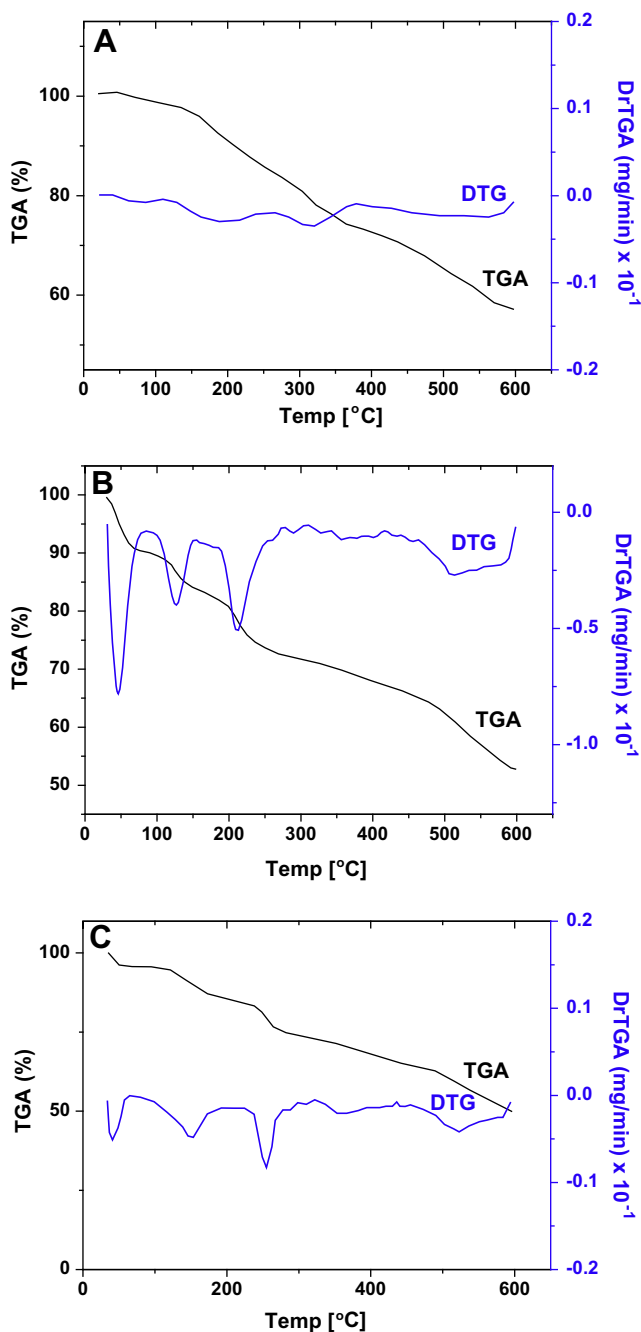


Fig. 10. TG curves of Cu(II), Co(II) and Ni(II)–H₂L complexes (A, B and C).

Table 4
Thermogravimetric data of Cu(II), Co(II) and Ni(II)/H₂L complexes.

Complexes	Steps	Temp. range (°C)	Decomposed assignments	Weight loss found (Calcd. %)
[Cu(H ₂ L)(H ₂ O) ₂ (Cl)]Cl	1st	25–120	–H ₂ O	3.19 (3.45)
	2nd	120–245	–H ₂ O + 1/2 Cl ₂	10.75(10.25)
	3rd	245–370	–Cl ₂	13.49(13.60)
	4th	370–600	Dec. H ₂ L	16.00(16.09)
	Residue	600	–	CuO
[Co(H ₂ L)(H ₂ O) ₃]Cl ₂ .3H ₂ O	1st	25–75	–3H ₂ O	9.31(9.16)
	2nd	75–165	–2H ₂ O	6.77(6.12)
	3rd	165–270	–½Cl ₂ + H ₂ O	9.00(9.08)
	4th and 5th	270–600	–Cl ₂ + Dec. H ₂ L	21.89(22.26)
	Residue	–	–	CoO
[Ni(H ₂ L)(H ₂ O) ₂]Cl ₂ .6H ₂ O	1st	25–70	–2H ₂ O	5.69(5.76)
	2nd	70–180	–3H ₂ O	9.08(8.64)
	3rd	180–270	–3H ₂ O	9.19(8.64)
	4th	270–375	–½Cl ₂	6.24(5.68)
	5th	375–600	Cl ₂ + Dec. H ₂ L	21.80(22.87)
Residue	–	–	NiO	

this complex has an octahedral feature. There are two detectable bands were observed at 22,222 cm^{−1} (strong intensity) nm and 28,169 cm^{−1} (very strong intensity) due to ⁴T_{1g} → ⁴A_{2g} and ⁴T_{1g} → ⁴T_{1g}(P) transition, respectively. The magnetic moment of Co(II) complex was found at 3.89 B.M. at room temperature which supported the octahedral geometry (Fig. 6).

The electronic spectrum of the orange yellow color complex of nickel(II) ion, [Ni(H₂L)(H₂O)₂]Cl₂.6H₂O, has a strong band at 22,472 cm^{−1} located inside the experimental value at (15,000–25,000 cm^{−1}) of square planar geometry. This band ascribe to ¹A_{1g} → ¹A_{2g} transition [29]. In literature survey the square planar complexes of nickel have been a color ranged from orange to red, this information matched with our nickel(II) complex. The magnetic measurements come also to confirm the square planar structure with a diamagnetic value. The structure of Ni(II) complex according to elemental analysis, infrared/Raman spectra and electronic spectra as well as magnetic moments can be designed as follows in Fig. 7.

3.4. ¹H NMR Spectral analysis

The ¹H NMR spectrum of H₂L Schiff base ligand was recorded to confirm the structural. The spectrum of H₂L ligand (Fig. 8) showed a (s, 1H) at δ = 15.284 ppm for NH proton, its down field appearance may be due to the participation of NH group in H-bonding with its neighboring nitrogen of azomethine group, (s, 1H) at δ = 10.220 ppm for OH group attached to C16 (Fig. 9), (s, 1H) at δ = 9.309 ppm for C9–H10 of azomethine group, (m, 11H) at δ = 6.994–8.322 ppm range for aromatic protons of the three aromatic rings and (s, 2H) at δ = 2.559 and 3.414 ppm for DMSO and H₂O/DMSO, respectively. The assignment for the spectrum peaks proposed the presence of free ligand in its hydrogen bonding between H(28)–N(7) (Fig. 9).

ions. This is indicating that, the azomethine group nitrogen atom appears to be coordinated to the metal ions [14].

The electronic spectrum of the dark green copper(II) complex, [Cu(H₂L)(H₂O)₂(Cl)]Cl, in DMSO solvent (Fig. 5) showed mainly transition bands at 22,727 cm^{−1} ascribe to ²E_g → ²T_{2g} transition in distorted octahedral geometry [28]. The other detectable band at 26,881 cm^{−1} was assigned to L → M charge transfer. The found value of the magnetic moment of Cu(II) complex was 1.76 B.M., which supported the octahedral feature [28].

Undertaken the phenomena that octahedral cobalt(II) complexes have a pink or reddish brown [28] but most tetrahedral Co(II) complexes have an intense blue or green color, herein the electronic spectrum of the dark brown, [Co(H₂L)(H₂O)₃]Cl₂.3H₂O, complex in DMSO solvent with 1.0 × 10^{−3} mol/cm³ showed that

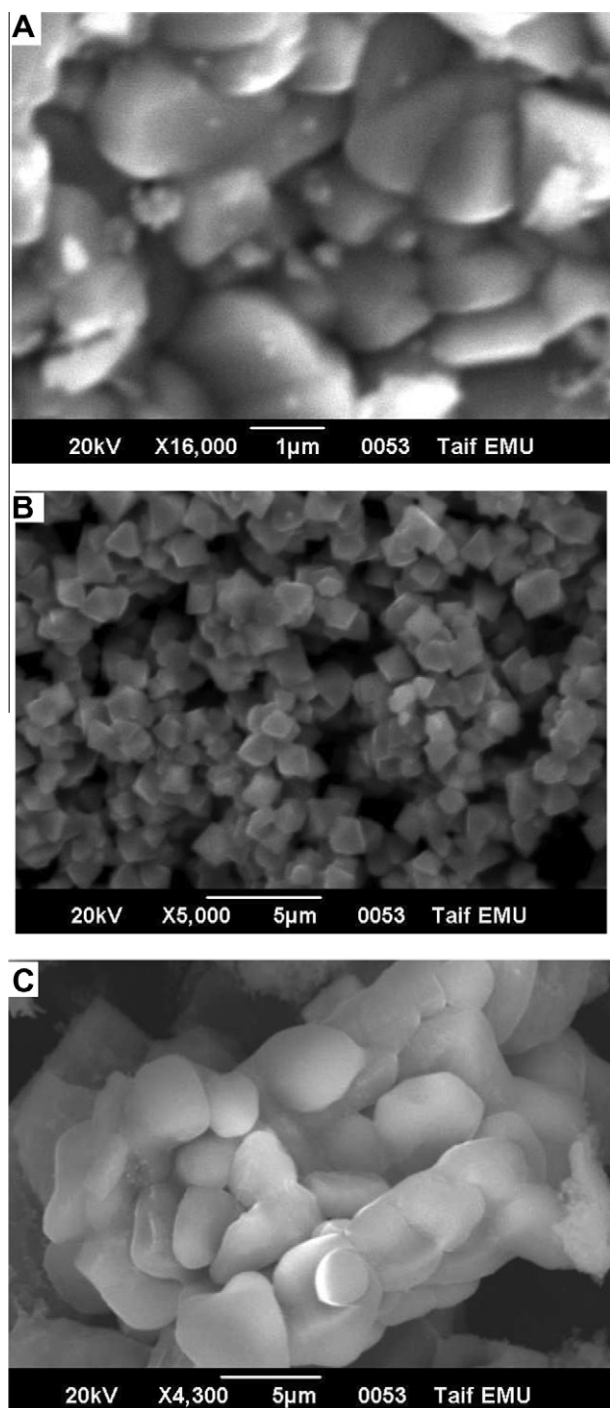


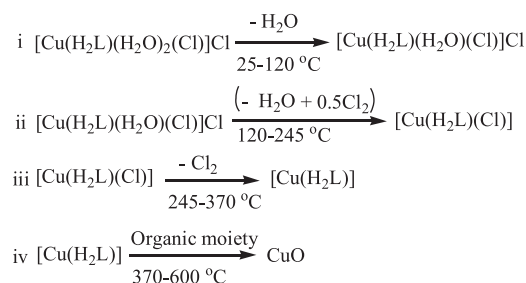
Fig. 11. SEM images of Cu(II), Co(II) and Ni(II)–H₂L complexes at 600 °C.

3.5. Thermal analysis

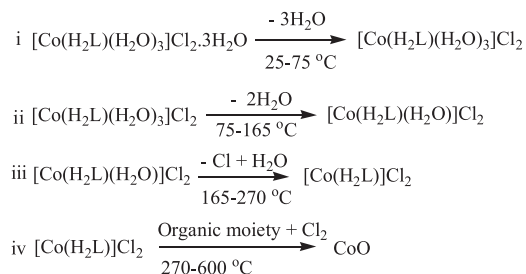
The TGA and DTG thermal curves of Cu(II), Co(II) and Ni(II) complexes of 2-[(5-*o*-chlorophenylazo-2-hydroxybenzylidene)amino]phenol Schiff base (H₂L) in nitrogen environment with a heating rate 10 °C/min are given in Fig. 10 and the decomposition steps are assigned in Table 4. The pathway of these complexes is the same sequences with overlapping steps vary from one complex to another as designed in the following Scheme 2.

Table 4 illustrated to the behavior of the thermal degradation according to TG curves for each step in the decomposition sequence of the Cu(II), Co(II) and Ni(II)–H₂L complexes. The mass

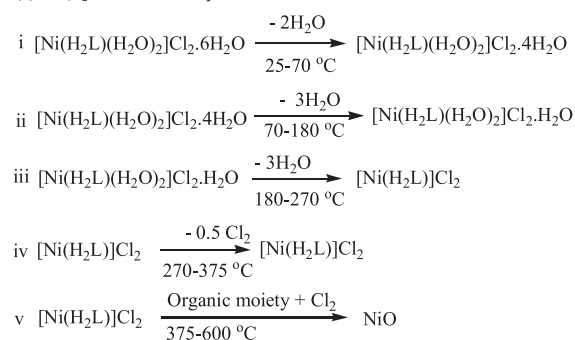
1- [Cu(H₂L)(H₂O)₂(Cl)]Cl complex



2- [Co(H₂L)(H₂O)₃]Cl₂·3H₂O complex



3- [Ni(H₂L)(H₂O)₂]Cl₂·6H₂O complex



Scheme 2. Thermal decomposition steps of Cu(II), Co(II) and Ni(II) complexes.

losses obtained from TG curves are in a good agreement with the calculated values. The first decomposition step of the [Cu(H₂L)–(H₂O)₂(Cl)]Cl complex occurs at the 25–120 °C range (Fig. 10) with a weak DTG maximum peak at 75 °C. This step is accompanied by weight loss (Obs. = 3.19%, Calc. = 3.45%) which assigned to the loss of one water molecules. The second step at 120–245 °C range with a weak DTG peak at 193 °C due to weight loss of (Obs. = 10.75%, Calc. = 10.25%) corresponds to the elimination of H₂O + 0.5Cl₂. The third decomposition step (DTG_{max} = 320 °C) located within the range of 245–370 °C with mass loss (Obs. = 13.49%, Calc. = 13.60%) and assigned to the evolved half chlorine molecule. The decomposition of H₂L ligand started above 370 °C with mass loss (Obs. = 16.00%, Calc. = 16.09%) and left CuO contaminated with carbon atoms.

The TG/DTG curve of [Co(H₂L)(H₂O)₃]Cl₂·3H₂O complex, a five decomposition steps were observed. The first and second steps in the range of 25–165 °C with DTG peaks at 45 and 125 °C, respectively, have a total weight loss (Obs. = 16.08%, Calc. = 15.28%). This temperature range is within the normal limit to that reported for the release of uncoordinated and coordinated water molecules. The third step within the range of (165–270 °C) with a medium strong DTG peak at 211 °C was assigned to the loss of (0.5Cl₂ + H₂O) molecules and the weight loss (Obs. = 9.00%, Calc. = 9.08%). In case of the fourth and fifth decomposition steps the total mass loss up to 270 °C is in agreement with the calculated values

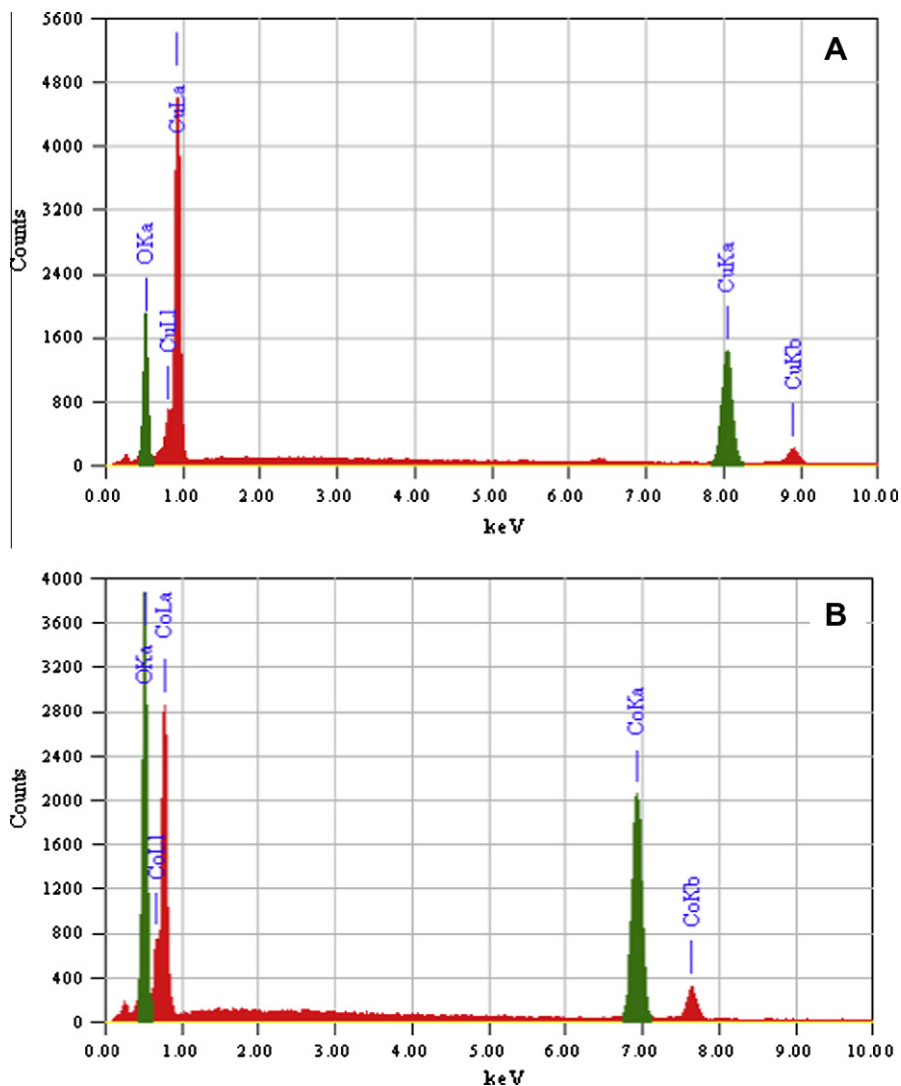


Fig. 12. The EDX analysis of (A) Cu(II) and (B) Co(II)—H₂L complexes at 600 °C.

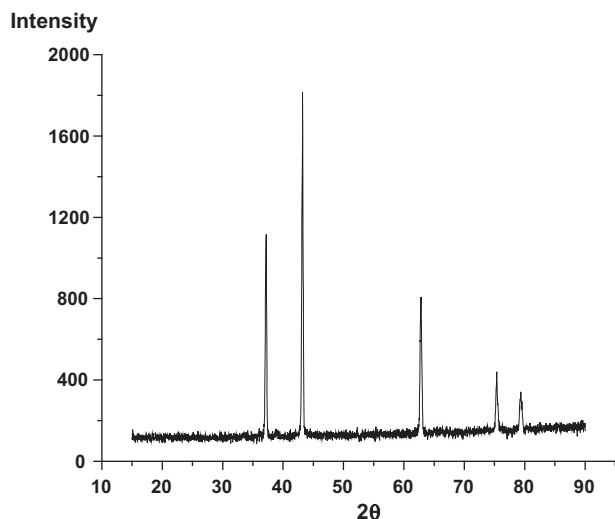


Fig. 13. The XRD spectrum of Ni(II)—H₂L complex at 600 °C.

Table 5

XRD spectral data of the highest value of intensity of the cobalt and nickel residuals at 600 °C.

Residuals	2θ	FWHM	Relative intensity	Particle size
Cobalt	37	0.170	100	51
Nickel	43	0.305	100	29

(Obs. = 21.89%, Calc. = 22.26%). The CoO as a final residual at 600 °C was checked using X-ray powder diffraction technique.

Concerning to [Ni(H₂L)(H₂O)₂]Cl₂·6H₂O complex the first-to-fifth steps of decomposition in TG curve occurs at 25–70 °C, 70–180 °C, 180–270 °C, 270–375 °C and 375–600 °C ranges with different temperatures of maximum DTG at 43, 152, 258, 362 and 527 °C, respectively. The weight loss of 1st (Obs. = 5.69%, Calc. = 5.76%), 2nd (Obs. = 9.08%, Calc. = 8.64%), 3rd (Obs. = 9.19%, Calc. = 8.64%), 4th (Obs. = 6.24%, Calc. = 5.68%), and 5th (Obs. = 21.80%, Calc. = 22.87%) were assigned to the loss of 2H₂O, 3H₂O, 3H₂O, 0.5Cl₂ and (0.5Cl₂ + decomposition of H₂L), respectively.

Table 6
Kinetic parameters using the Coats–Redfern (CR) and Horowitz–Metzger (HM) equations for the Cu(II), Co(II) and Ni(II)–H₂L complexes.

Complex	Stage	Method	Parameter					r
			E (J mol ⁻¹)	A (s ⁻¹)	ΔS (J mol ⁻¹ K ⁻¹)	ΔH (J mol ⁻¹)	ΔG (J mol ⁻¹)	
Cu(II)	3rd	CR	7.39 × 10 ⁴	1.60 × 10 ⁴	-1.70 × 10 ²	6.90 × 10 ⁴	1.70 × 10 ⁵	0.9951
		HM	8.49 × 10 ⁴	2.26 × 10 ⁵	-1.48 × 10 ²	8.00 × 10 ⁴	1.68 × 10 ⁵	0.9934
Co(II)	3rd	CR	1.03 × 10 ⁵	1.20 × 10 ⁹	-7.51 × 10 ¹	9.95 × 10 ⁴	1.36 × 10 ⁴	0.9977
		HM	1.09 × 10 ⁵	9.63 × 10 ⁹	-5.78 × 10 ¹	10.5 × 10	1.33 × 10 ⁴	0.9957
Ni(II)	3rd	CR	8.34 × 10 ⁴	9.88 × 10 ⁵	-1.35 × 10 ²	7.90 × 10 ⁴	1.51 × 10 ⁵	0.9825
		HM	9.26 × 10 ⁴	1.32 × 10 ⁷	-1.13 × 10 ²	8.82 × 10 ⁴	1.48 × 10 ⁵	0.9791

3.6. XRD and SEM/EDX studies

The aim of this paper beside the synthesis and characterization of the novel Schiff base and its Cu(II), Co(II) and Ni(II) complexes is to study of the final thermal decomposition products at 600 °C. These residuals were checked using scanning electron microscopy (SEM), energy-dispersive X-ray spectroscopy (EDX) and X-ray diffraction (XRD) techniques.

SEM is a simple method can be used to check the deposited samples which clearly indicated that the nanoparticles have been formed. According to the images of SEM, the diameters of the residual samples for Cu(II), Co(II) and Ni(II) are about 400, 250 and 480 nm, respectively. Fig. 11 shows the scanning electron microscopy pictures of Cu(II), Co(II) and Ni(II)–H₂L particles at 600 °C. By comparison between the residual products in this study and the copper(II), cobalt(II) and nickel(II) oxides nanoparticles in the literature [30,31], it is obvious that the particles (250–480 nm diameters) are smaller and the Schiff base ligands can be used as a good precursors.

The results by energy dispersive X-ray analysis (EDX) have indicated that there are copper, cobalt and oxygen peaks, which meant there were oxygen contamination or the deposited products were copper or cobalt oxides as shown in Fig. 12.

The X-ray powder diffraction patterns in the range of 10° < 2θ < 90° for the residual products at 600 °C were carried in order to obtain an idea about the lattice dynamics of the resulted oxides of cobalt and nickel. X-ray diffraction of the residual products of cobalt and nickel H₂L complexes were recorded between 10° and 90° 2θ and are given in Fig. 13. The values of 2θ, full width at half maximum (FWHM) of prominent intensity peak, relative intensity and particle size of cobalt and nickel residual products were compiled in Table 5. The crystallite size of the cobalt and nickel residuals at 600 °C could be estimated from XRD patterns by applying FWHM of the characteristic peaks using Deby–Scherrer equation (1) [32].

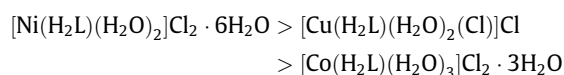
$$D = K\lambda/\beta\cos\theta \quad (1)$$

where *D* is the particle size of the crystal gain, *K* is a constant (0.94 for Cu grid), *λ* is the X-ray wavelength (1.5406 Å), *θ* is the Bragg diffraction angle and *β* is the integral peak width. The particle size was estimated according to the highest value of intensity compared with the other peaks. The particle size for the cobalt and nickel thus obtained were 51 and 29 nm, respectively. These data gave an impression that the particle size located within nano-scale range.

3.7. Kinetic parameters

The kinetic studies upon the thermal degradation processes are a powerful indication to provide sufficient knowledge about Arrhenius parameters viz. activation energy (*E*^{*}), frequency factor (*A*), enthalpy of activation (*H*^{*}), entropy of activation (*S*^{*}) and free energy of activation (*G*^{*}). From TG/DTG curves, Coats–Redfern and Horowitz–Metzger [33,34] were employed to calculate mentioned

kinetic parameters. The data was summarized and tabulated in Table 6. In fact the increasing in (*A*) value led to decreasing in (*E*^{*}), so, when the activation energy has a higher value the thermal stability increased. The higher values of (*E*^{*}) and lower values of (*A*) are supported the reaction to proceed slower than normal [35,36]. This fact has been applicable for the H₂L complexes studied in the present paper. So, the following order of thermal stability has been sequences as follows:



The negative values of (*S*^{*}) indicate that the activated complex has a more ordered [37] than that of either the reactants. The values of both *E*^{*} and *H*^{*} are equivalent.

4. Conclusion

A novel tridentate Schiff base ligand derived from condensation of aminophenol and 5-arylaazo-salicylaldehyde and its copper(II), cobalt(II) and nickel(II) complexes have been characterized by spectroscopic techniques. The calcinations of the Cu(II), Co(II) and Ni(II)–H₂L at 600 °C have succeeded in synthesized nano-structured of Ni and Co oxides nanoparticles. The micro/nano-structures and the composition of the residuals nanoparticles have been studied using SEM, EDX and XRD. The particles deposited at calcinations temperature (600 °C) which is in the region of 250–480 nm in diameters.

Acknowledgement

The author express a lot of thanks for prof. I.M. El-Deen, Department of Chemistry, Faculty of Science, Port Said University for his assistance in saving the Schiff base compound used in this study.

References

- [1] S.C. Bell, G.L. Conklin, S.J. Childress, J. Am. Chem. Soc. 85 (1963) 2868.
- [2] H.A. El-Borae, J. Therm. Anal. Calorim. 81 (2005) 339.
- [3] Z.M. Zaki, S.S. Haggag, A.A. Sayed, Spectrosc. Lett. 31 (1998) 757.
- [4] G. Kumar, D. Kumar, C.P. Singh, A. Kumar, V.B. Rana, J. Serb. Chem. Soc. 75 (5) (2010) 629.
- [5] V.K. Aghera, P.H. Parsania, J. Sci. Ind. Res. 67 (2008) 1083.
- [6] N. Raman, V. Muthuraj, S. Ravichandran, A. Kulandaisamy, J. Chem. Sci. 115 (3) (2003) 161.
- [7] V.P. Lozitsky, V.E. Kuzmin, A.G. Artemenko, R.N. Lozitska, A.S. Fedtchouk, E.N. Muratov, A.K. Mescheriakov, SAR QSAR Environ. Res. 16 (2005) 219.
- [8] D. Sinha, A.K. Tiwari, S. Singh, G. Shukla, P. Mishra, H. Chandra, A.K. Mishra, Eur. J. Med. Chem. 43 (2008) 160.
- [9] S. Adsule, V. Barve, D. Chen, F. Ahmed, Q.P. Dou, S. Padhye, F.H. Sarkar, J. Med. Chem. 49 (2006) 7242.
- [10] S. Ren, R. Wang, K. Komatsu, P. Bonaz-Krause, Y. Zyrianov, C.E. McKenna, C. Csipke, Z.A. Tokes, E.J. Lien, J. Med. Chem. 45 (2002) 410.
- [11] E.A. Elzahany, K.H. Hegab, S.K.H. Khalil, N.S. Youssef, Aust. J. Basic Appl. Sci. 2 (2008) 210.
- [12] F.M. Morad, M.M. El-Ajaily, S. Ben Gweirif, J. Sci. Appl. 1 (2007) 72.
- [13] V.S. Kshirsagar, A.C. Garade, R.B. Mane, K.R. Patil, A. Yamaguchi, M. Shirai, C.V. Rode, Appl. Catal. A 370 (1–2) (2009) 16.

- [14] M.S. Refat, I.M. El-Deen, H.K. Ibrahim, S. El-Ghool, *Spectrochim. Acta Part A Mol. Biomol. Spectrosc.* 65 (2006) 1208.
- [15] S. Brooker, S.S. Iremonger, P.G. Plieger, *Polyhedron* 22 (5) (2003) 665.
- [16] H.E. Katz, K.D. Singer, J.E. Sohn, C.W. Dirk, L.A. King, H.M. Gordon, *J. Am. Chem. Soc.* 109 (21) (1987) 6561.
- [17] T. Abe, S. Mano, Y. Yamada, A. Tomotake, *J. Image. Sci. Technol.* 43 (1999) 339.
- [18] S. Wang, S. Shen, H. Xu, *Dyes Pigments* 44 (2000) 195.
- [19] K. Maho, T. Shintaro, K. Yutaka, W. Kazuo, N. Toshiyuki, T. Mosahiko, *Jpn. J. Appl. Phys.* 42 (2003) 1068.
- [20] A.A. Khandar, Z. Rezvani, *Polyhedron* 18 (1999) 129.
- [21] R.J. Fessenden, J.S. Fessenden, *Inorganic Chemistry*, fourth ed., Springer, Berlin, 1990, p. 587.
- [22] A.I. Vogel, *A Text Book of Quantitative Inorganic Analysis*, Longmans, London, 1994.
- [23] W.J. Geary, *Coord. Chem.* 7 (1971) 81.
- [24] S. Sarawat, G.S. Srivastava, R.C. Mehrotra, *J. Organomet. Chem.* 129 (1977) 155.
- [25] G. Wang, J.C. Chang, *Synth. Inorg. Met. – Org. Chem.* 2 (4) (1994) 1091.
- [26] K. Nakamoto, *Infrared Spectra of Inorganic and Coordination Compounds*, Wiley, New York, 1970.
- [27] J.R. Platt, *J. Chem. Phys.* 17 (1949) 484.
- [28] A.B.P. Lever, *Inorganic Electronic Spectroscopy*, second ed., Elsevier, Amsterdam, 1997.
- [29] A.A.A. Emara, *Spectrochim. Acta Part A Mol. Biomol. Spectrosc.* 77 (1) (2010) 117.
- [30] M. Salavati-Niasari, F. Mohandes, F. Davar, M. Mazaheri, M. Monemzadeh, N. Yavarinia, *Inorg. Chim. Acta* 362 (2009) 3691.
- [31] B.P. Baranwal, T. Fatma, A. Varma, A.K. Singh, *Spectrochim. Acta Part A Mol. Biomol. Spectrosc.* 75 (2010) 1177.
- [32] C.X. Quan, L.H. Bin, G.G. Bang, *Mater. Chem. Phys.* 91 (2005) 317.
- [33] A.W. Coats, J.P. Redfern, *Nature* 201 (1964) 68.
- [34] H.W. Horowitz, G.A. Metzger, *Anal. Chem.* 35 (1963) 1464.
- [35] S.S. Sawney, A.K. Bausal, *Thermochim. Acta* 66 (1983) 347.
- [36] P. Chourasia, K.K. Suryesh, A.P. Mishra, *Proc. Ind. Acad. Sci.* 105 (1993) 173.
- [37] A.A. Frost, R.G. Pearson, *Kinetics and Mechanism*, New York, Wiley, 1961.